

Experimental demonstration of propagating plasmons in metallic nanoshells

Md M. Hossain,¹ Alessandro Antonello,² and Min Gu^{1,*}

¹Centre for Micro-Photonics and CUDOS, Faculty of Engineering and Industrial Sciences, Swinburne University of Technology, Hawthorn, Victoria 3122, Australia

²IOM-CNR, INSTM and Dipartimento di Ingegneria Meccanica, Settore Materiali, Università di Padova, Via Marzolo 9, 35131 Padua, Italy
mgu@swin.edu.au

Abstract: In this paper, we show the experimental demonstration of plasmon propagation in cylindrical metallic nanoshells which is coated, via the electroless silver deposition method, on dielectric nanorods fabricated by using the direct laser writing method. The experimental measurement and the numerical analysis reveal the polarization sensitivity of the plasmon modes within the nanoshells. We further characterize the fundamental properties of these plasmon modes by exploiting their dispersive features and explain the mechanism for the excitation of the plasmon modes by identifying their radiative and nonradiative nature.

©2012 Optical Society of America

OCIS codes: (250.5403) Plasmonics; (310.6628) Subwavelength structures, nanostructures.

References and links

1. E. Prodan, C. Radloff, N. J. Halas, and P. Nordlander, "A hybridization model for the plasmon response of complex nanostructures," *Science* **302**(5644), 419–422 (2003).
2. E. Prodan and P. Nordlander, "Plasmon hybridization in spherical nanoparticles," *J. Chem. Phys.* **120**(11), 5444–5454 (2004).
3. C. Radloff and N. J. Halas, "Plasmonic properties of concentric nanoshells," *Nano Lett.* **4**(7), 1323–1327 (2004).
4. A. Moradi, "Plasmon hybridization in metallic nanotubes," *J. Phys. Chem. Solids* **69**(11), 2936–2938 (2008).
5. M. D. Turner, M. M. Hossain, and M. Gu, "The effects of retardation on plasmon hybridization within metallic nanostructures," *New J. Phys.* **12**(8), 083062 (2010).
6. J. Li, M. M. Hossain, B. Jia, D. Buso, and M. Gu, "Three-dimensional hybrid photonic crystals merged with localized plasmon resonances," *Opt. Express* **18**(5), 4491–4498 (2010).
7. M. M. Hossain, M. D. Turner, and M. Gu, "Ultrahigh nonlinear nanoshell plasmonic waveguide with total energy confinement," *Opt. Express* **19**(24), 23800–23808 (2011).
8. E. Nicoletti, D. Bulla, B. Luther-Davies, and M. Gu, "Generation of $\lambda/12$ nanowires in chalcogenide glasses," *Nano Lett.* **11**(10), 4218–4221 (2011).
9. M. D. Turner, G. E. Schröder-Turk, and M. Gu, "Fabrication and characterization of three-dimensional biomimetic chiral composites," *Opt. Express* **19**(10), 10001–10008 (2011).
10. A. Antonello, B. Jia, Z. He, D. Buso, G. Perotto, L. Brigo, G. Brusatin, M. Guglielmi, M. Gu, and A. Martucci, "Optimized electroless silver coating for optical and plasmonic applications," *Plasmonics* (Published online: March 18, 2012), DOI: 10.1007/s11468-012-9352-6
11. G. Dolling, M. Wegener, and S. Linden, "Realization of a three-functional-layer negative-index photonic metamaterial," *Opt. Lett.* **32**(5), 551–553 (2007).
12. A. W. Snyder and J. D. Love, *Optical Waveguide Theory* (Chapman & Hall, London, New York, 1983).
13. T. Nikolajsen, K. Leosson, and S. I. Bozhevolnyi, "Surface plasmon polariton based modulators and switches operating at telecom wavelengths," *Appl. Phys. Lett.* **85**(24), 5833–5835 (2004).
14. C. Min and G. Veronis, "Absorption switches in metal-dielectric-metal plasmonic waveguides," *Opt. Express* **17**(13), 10757–10766 (2009).
15. J. A. Dionne, K. Diest, L. A. Sweatlock, and H. A. Atwater, "PlasMOSstor: a metal-oxide-Si field effect plasmonic modulator," *Nano Lett.* **9**(2), 897–902 (2009).
16. W. Cai, J. S. White, and M. L. Brongersma, "Compact, high-speed and power-efficient electrooptic plasmonic modulators," *Nano Lett.* **9**(12), 4403–4411 (2009).
17. R. F. Oulton, V. J. Sorger, T. Zentgraf, R. M. Ma, C. Gladden, L. Dai, G. Bartal, and X. Zhang, "Plasmon lasers at deep subwavelength scale," *Nature* **461**(7264), 629–632 (2009).

18. M. T. Hill, Y. S. Oei, B. Smalbrugge, Y. Zhu, T. De Vries, P. J. Van Veldhoven, F. W. M. Van Otten, T. J. Eijkemans, J. P. Turkiewicz, H. De Waardt, E. J. Geluk, S. H. Kwon, Y. H. Lee, R. Nötzel, and M. K. Smit, "Lasing in metallic-coated nanocavities," *Nat. Photonics* **1**(10), 589–594 (2007).
-

1. Introduction

Metallic nanoparticles and patterned metallic nanostructures with certain geometries can support resonant plasmon modes. In conductive nanoshells plasmons from inner and outer surfaces of the nanoshells can couple and form hybrid plasmon modes [1, 2]. Localized hybrid plasmon modes have been found in spherical metallic nanoshells with embedded dielectric cores [1, 3]. Later, it has been shown that hybrid plasmon modes can also exist in cylindrical metallic nanoshells [4, 5]. These plasmon modes can either be stationary or propagating (having a nonzero propagating wavevector along the axis of the metallic nanoshell cylinder) in nature [4, 5]. The existence of the stationary plasmon modes in cylindrical metallic nanoshells has been experimentally demonstrated through the observation of the enhanced optical absorption in three-dimensional hybrid photonic crystals stacked by the nanoshell cylinders [6]. However, it is the propagating nature of the plasmon mode that can play a key role in nanoscale waveguides, which is yet to be confirmed by experimental studies. In fact, one of the potential applications of the propagating plasmons is the generation of the ultrahigh nonlinear plasmonic waveguides with total energy confinement within the cylindrical metallic nanoshells, as predicated recently [7].

In this work, as a key step towards the realization of metallic nanoshell plasmonic devices, we report on the experimental confirmation of the propagating plasmon modes within elliptical nanoshell plasmonic waveguides fabricated by the direct laser writing (DLW) and electroless silver deposition method. We also support our experimental findings with detailed numerical characterization. The plasmon modes within the metallic nanoshells are highly polarization sensitive and here we successfully characterize the polarization sensitivity with the excitations of linearly polarized (TE and TM) lights in the experimental measurements and numerical calculations. Furthermore, our detailed theoretical analysis of the dispersive properties reveals that the physical mechanism for the excitation of the propagating plasmons within the experimental measurements is associated with the radiative nature of the plasmon modes.

2. Experimental methods

The DLW fabrication method can be employed to fabricate subwavelength dielectric nanowires in linear [6] and nonlinear materials [8]. The nanoshell plasmonic waveguides studied in this paper comprise an array of dielectric nanorods coated by metallic nanoshells. For the fabrication of the dielectric nanorods by DLW [9], a beam of femtosecond (~150 fs) laser pulses at a repetition rate of 76 MHz and at a wavelength of 580 nm was focused into the commercial liquid photoresist IP-L (Nanoscribe GmbH) with an oil-immersion high NA objective (Olympus, NA = 1.4, 100 \times). The dielectric nanorod array was written by the 3D translation of the liquid photoresist mounted on a piezoelectric scanning stage (P562, Physik Instrumente). The cross-section of the dielectric nanorods possesses an elliptical shape as the optical intensity distribution in the focal spot of the high NA objective creates elongated shape in the axial direction during the DLW fabrication. The nanorod array was supported by two massive frames at the two ends of the nanorods of a length of 15 μm , as shown in Fig. 1. A thinner frame was also fabricated at the middle of the dielectric rods for further mechanical stability. The array had a periodicity of 3.0 μm to avoid the interaction between the rods.

We adopted an electroless silver deposition method to deposit a thin metallic coating composed of silver nanoparticles on the dielectric nanorods surfaces. This deposition method is based on the modified Tollens reaction [10]. The densely packed silver nanoparticles in the electroless deposition have sizes in the range of 40 to 50 nm with a mean crystalline silver diameter of 43 nm [10]. Hence, the effective thickness of the silver film is assumed as 37 nm.

The silver nanoparticles in the film were well connected, assuring high electrical conductivity. Figure 1 shows a scanning electron microscopy (SEM) image of an array of the fabricated dielectric rods coated by a thin homogeneous silver film. These coated nanorods behave as nanoshell plasmonic waveguides.

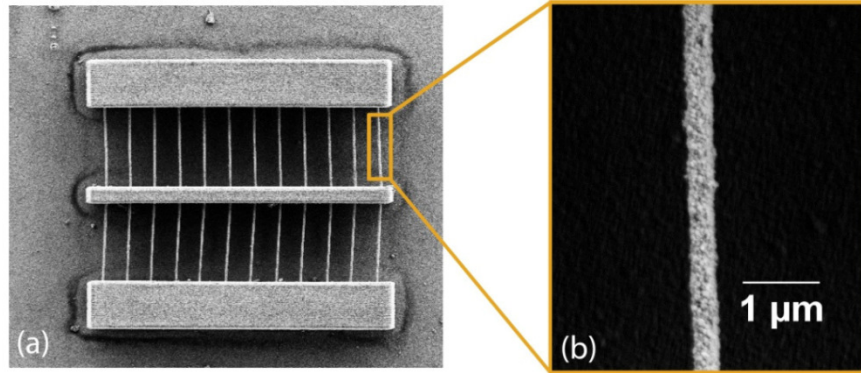


Fig. 1. (a) SEM image of an electroless silver coated polymer rod array (b) Magnified view of the silver nanoparticles coated polymer rods.

Experimental characterization of the reflection spectra of the nanoshell plasmonic waveguides were performed by using a Nicolet Nexus Fourier-transform infrared (FTIR) spectrometer with a continuum infrared microscope (Thermo Nicolet, Madison, Wisconsin, USA). The reflective 32x NA 0.65 objective (Reflachromat, Thermo Nicolet) provided a hollow light cone with an angle range of 18° to 41° . Though such a characterization setup should be applicable for transmission measurement, the inability of the selectivity of the electroless silver coating method led to the deposition of the silver film to the glass substrate beneath the dielectric rod gratings and hence, restricted any transmission measurement by the FTIR microscopy. Reflection measurements were instead carried out for linearly polarized incident light.

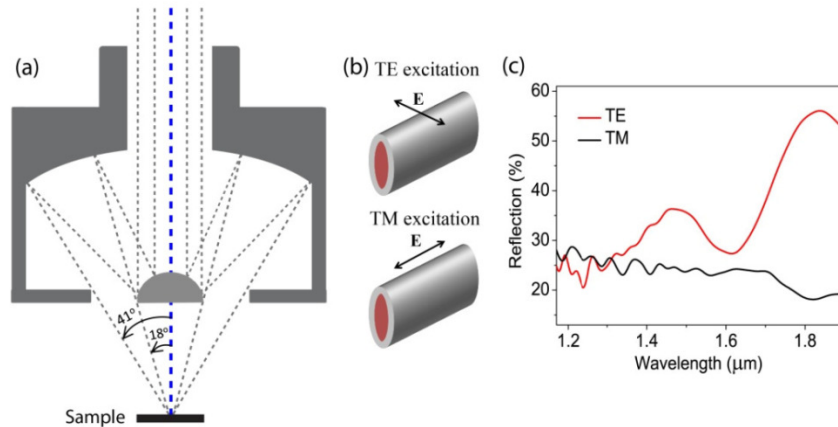


Fig. 2. FTIR microscopy measurements for the reflection spectra with the two orthogonal linearly polarized incident beams. (a) Schematic illustration of the cross-section of the reflective FTIR microscope objective, symmetric around its axis (blue dashed line), depicting the hollow light cone (18° to 41°). (b) The excitation scheme of the plasmon mode of the nanoshell plasmonic waveguide for TE (electric fields perpendicular to the nanoshell cylinder axis) excitation and TM (electric field parallel to the nanoshell cylinder axis) excitation (c) The TE measurement shows a reflection dip at $\lambda = 1.615 \mu\text{m}$. The TM measurement does not show such a phenomenon.

Figure 2(c) shows that the reflection spectra for the TE measurement possess a reflection dip at the wavelength of 1.615 μm . However, for the TM measurement no such reflection dip was observed. We argue that the resonant reflection dip for the TE measurement is due to the optical absorption caused by the propagating plasmons on the surface of the silver nanoshells, which is supported by the theoretical calculation detailed in the next section. Some small oscillations also appear in the measurement at the short wavelengths region (between 1.17 μm to 1.35 μm) which are due to the noisy spectral response of the FTIR detector and do not contribute to any significant physical insight.

3. Numerical characterization

To understand the experimental results, we investigated the propagating plasmon mode characteristics of the cylindrical metallic nanoshell plasmonic waveguide with a subwavelength linear dielectric core. The refractive index of the linear dielectric core was set to 1.52 and the dispersive properties of the silver metal were expressed by the Drude model with plasma frequency $\omega_p = 1.37 \times 10^{16} \text{s}^{-1}$ and the collision frequency $\omega_c = 8.5 \times 10^{13} \text{s}^{-1}$ [11]. Commercially available finite-element based eigenmode solver (COMSOL Multiphysics) was used to extract the eigenmodes of the nanoshell plasmonic waveguide.

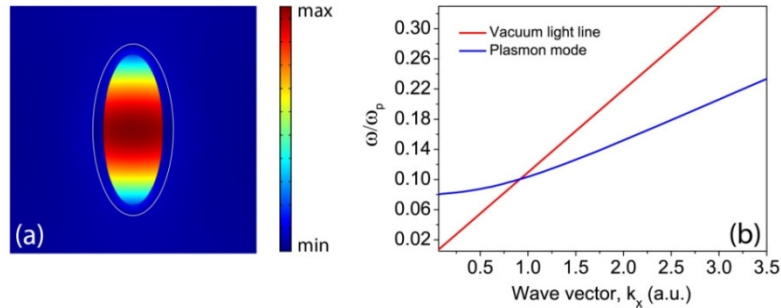


Fig. 3. (a) Calculated electric field distributions of the plasmon mode at $\lambda = 1.619 \mu\text{m}$ for the silver film coated dielectric nanorods with a core width of 220 nm, a core height of 550 nm and a silver nanoshell thickness of 37 nm thickness. The white line illustrates the boundary between the silver nanoshell and the air background. (b) Dispersion relation of the plasmon mode of the silver film coated nanorods for the same parameters used in (a).

Figure 3(a) shows the plasmon mode characteristics within the nanoshell plasmonic waveguide. The effective mode index $n_{\text{eff}} (k_{\text{mode}}/k_0$ [12]) is 0.50. The effective mode index $n_{\text{eff}} < 1$ states that the plasmon mode wavevector k_{mode} is lower in magnitude than the free space wavevector k_0 . The fundamental characteristics of such modes can be further understood from their dispersion relations. The dispersion curves presented in Fig. 3(b) depicts that the plasmon modes on the right hand side of the vacuum light line (with $k_{\text{mode}} > k_0$) are nonradiative while the plasmon modes staying on the left side of the vacuum light line (with $k_{\text{mode}} < k_0$) are radiative in nature. Thus these radiative modes with $n_{\text{eff}} < 1$ can be termed as leaky modes and can be excited externally.

The excitation scheme is demonstrated in Fig. 4(a). To excite the plasmon modes, the incident wave polarization needs to match with the plasmon mode polarization. An incident TE wave with the perpendicular incidence to the cylindrical nanoshell waveguide does not contain any wavevector component along the waveguide axis to excite the propagating plasmon modes ($k_{\text{mode}} \neq 0$); rather, it excites the stationary plasmon mode ($k_{\text{mode}} = 0$). However, an incident TE wave with an angle to the perpendicular direction provides wavevector component k_x (where $k_x < k_0$) along the nanoshell waveguide axis and thus can efficiently excite the propagating plasmon modes with $k_{\text{mode}} = k_x$ as shown in Fig. 4(a). For an incidence with angle θ , the incident radiation contains a wavevector component $k_x = k_0 \sin \theta$.

The excited plasmon modes decay over their propagation lengths and thus create absorption peaks of the incident radiations.

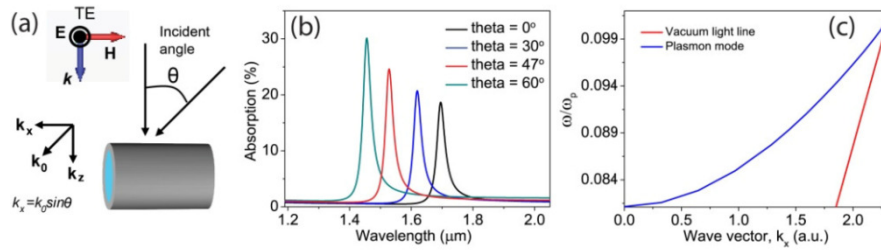


Fig. 4. (a) Schematic of the angle of incidence excitation of the propagating plasmon modes with the parallel component k_x of the incident wavevector k_0 . (b) Absorption peaks of the incident radiation with different incident angles. (c) The dispersion relation for the plasmon modes.

To confirm this we ran transmission/reflection calculations for the nanoshell plasmonic waveguides based on the finite element numerical simulations with the commercially available CST MWS software and record any absorption peaks within the spectra. The incident wave was a TE mode and the angle of incidence was varied over a range. It can be seen in Fig. 4(b) that absorption peaks arise due to the excitation of the propagating plasmon modes by the external EM radiation with oblique incidence. For normal incidence ($\theta = 0$) with $k_x = 0$, only the stationary plasmon mode is excited but for an oblique incidence ($\theta \neq 0$) the nonzero wavevector component k_x matches the propagating plasmon wavevector k_{mode} and thus excites it. It should be noted that as we continuously increase the incident angle θ , k_x increases and excites the high frequency plasmon modes. For an incidence angle of $\theta = 30^\circ$, the plasmon resonance occurs at the wavelength of $1.619 \mu\text{m}$, with a plasmon mode effective index, n_{eff} of 0.50 ($n_{\text{eff}} = k_{\text{mode}}/k_0 = k_0 \sin 30^\circ/k_0$). This exactly matches the effective mode index of the plasmon mode calculated by the eigenmode solver at the wavelength of $1.619 \mu\text{m}$ as shown in Fig. 3(a) and thus confirms the validity of our theoretical calculations.

Figure 4(c) shows the dispersion relation for the propagating plasmons with the wavevector components k_x extracted from the calculated spectral positions of the absorption peaks for different incidence angles. The dispersion curve for the plasmon modes with $k_x < k_0$ exactly replicates the dispersive features of the plasmon modes at the left hand side of the light line presented in Fig. 3(b) confirming their radiative nature. Furthermore, to confirm the polarization sensitivity of the plasmon modes, we also ran simulations for TM waves with oblique incidence. No such absorption peaks were observed. This is due to the fact that for the oblique incidence with a TM wave, although the incident wave carries a wavevector component k_x along the nanoshell waveguide axis, it does not match the polarization of the plasmon mode and hence does not excite this mode.

Now, to compare with our experimental results, we recall from Fig. 2(c) that a reflection dip at $1.615 \mu\text{m}$ exists for the TE mode in the experimentally measured reflection spectra of the silver coated dielectric rod array. As the measurement was carried out for an opening angle of 18° to 41° , we assume that the mid spectral position for the absorption peak would occur at the 30° angle of incidence. Indeed, it can be noticed from the theoretically calculated results presented in Fig. 4(b) that for a 30° angle of incidence excitation of the propagating plasmon mode, the optical absorption occurs at $1.619 \mu\text{m}$. This is a good agreement between the experiment and the theory. The slight deviation of the measured spectra from the simulated results originates from the averaging effects of the measurements over the wide and finite opening angle of the FTIR measurements and the roughness of the deposited silver film consisting of the finite-sized silver nanoparticles. Furthermore, the supporting frame ($3.0 \mu\text{m}$ thick) fabricated at the middle of the grating sample and coated with silver as shown in Fig.

1(a) can act as a scattering source and drastically weaken the reflection signal measured by the FTIR microscope detector.

4. Conclusion

In conclusion, we have experimentally demonstrated the existence of the propagating plasmon modes in cylindrical metallic nanoshells. It has also been demonstrated that the combination of the DLW and electroless silver deposition methods is an effective way to realize nanoshell plasmonic waveguides. Both the experimental and theoretical studies show that the propagating plasmon modes within the nanoshell plasmonic waveguides can be excited by a TE wave. These results are important steps towards the realization of the nonlinear nanoshell plasmonic waveguides [7] which has potential applications in nonlinear optical switching [13, 14], plasmonic modulation [15, 16] and nano-lasers [17, 18].

Acknowledgment

This research was conducted by the Australian Research Council Centre of Excellence for Ultrahigh bandwidth Devices for Optical Systems (project number CE110001018). Md M. Hossain also acknowledges the useful scientific discussions with Mark Turner.